

Supporting Information

Secondary nanoplastics released from a biodegradable microplastic severely impact freshwater environments

Miguel González-Pleiter,^{1*†} Miguel Tamayo-Belda,^{1†} Gerardo Pulido-Reyes,¹ Georgiana Amariei,² Francisco Leganés,¹ Roberto Rosal,² Francisca Fernández-Piñas¹

1. Department of Biology, Faculty of Science, Universidad Autónoma de Madrid, E-28049, Madrid, Spain

2. Department of Chemical Engineering, Universidad de Alcalá, E-28871 Alcalá de Henares, Madrid, Spain

* The corresponding author

† These authors contributed equally to this work

Corresponding Author: mig.gonzalez@uam.es

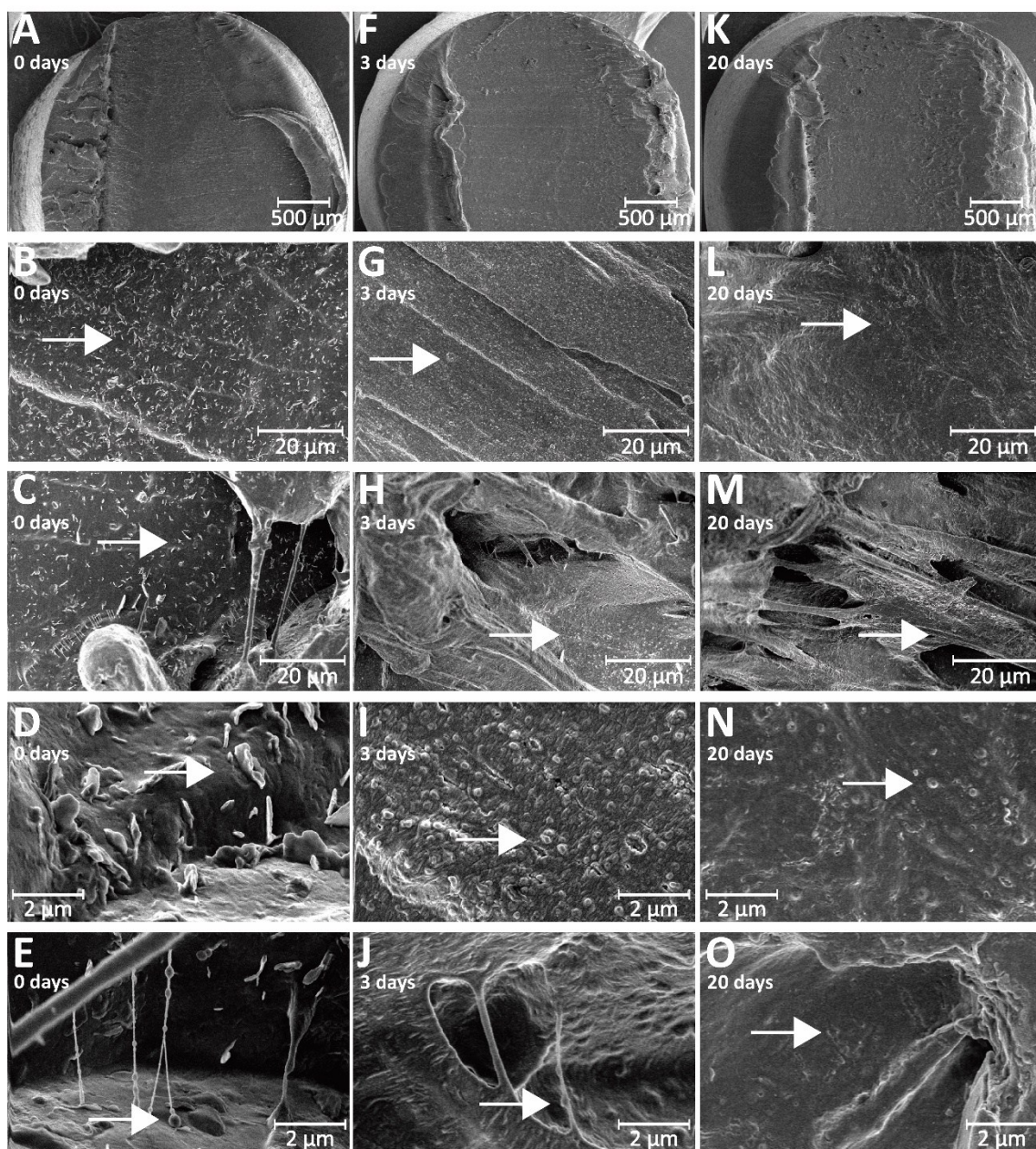


Fig. S1. SEM images of surface smoothing of PHB-microplastics abiotically degraded in MilliQ water buffered with 2 mM phosphate (pH 7.0) at 28 °C in constant shaking (135 rpm) during: 0 days (A-E), 3 days (F-J) and 20 days (K-O) and at 3 different magnifications (74x, 3000x and 25000x; scale bars included). At higher magnifications white arrows indicate representative structures of the smoothing process at each degradation time, in both the micrometric range, studied at 3000x (B, C, G, H, L and M), and the nanometric range, studied at 25000x (D, E, I, J, N and O).

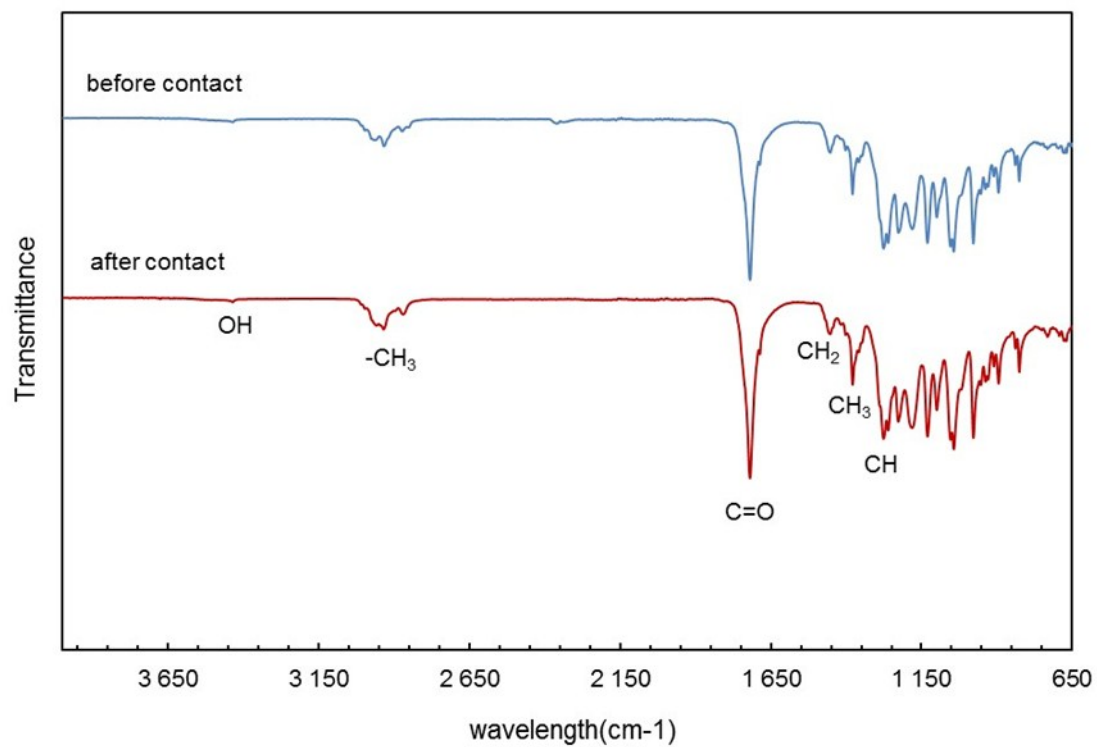


Fig. S2. ATR-FTIR of PHB-microplastics before and after 3 days of abiotic degradation.

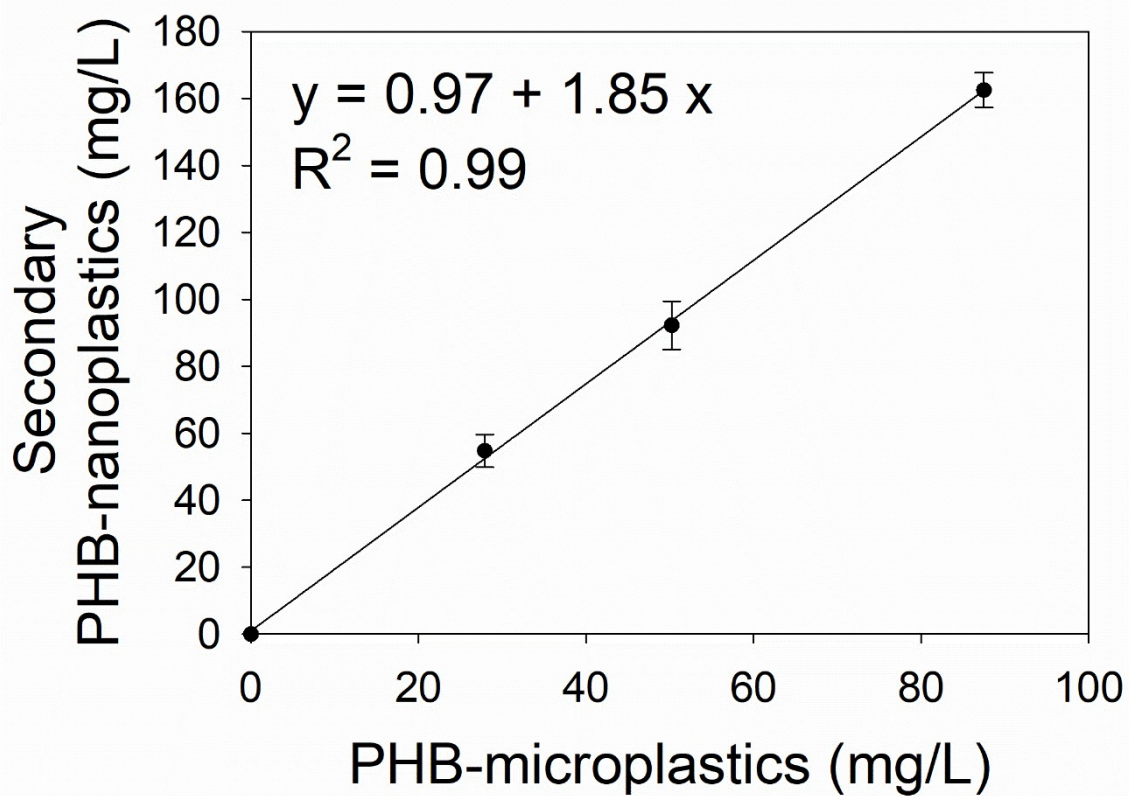


Fig. S3. Concentration of secondary PHB-nanoplastics released from different initial concentration of PHB-microplastics (25, 50 and 100 mg/L) after 3 days of abiotic degradation.

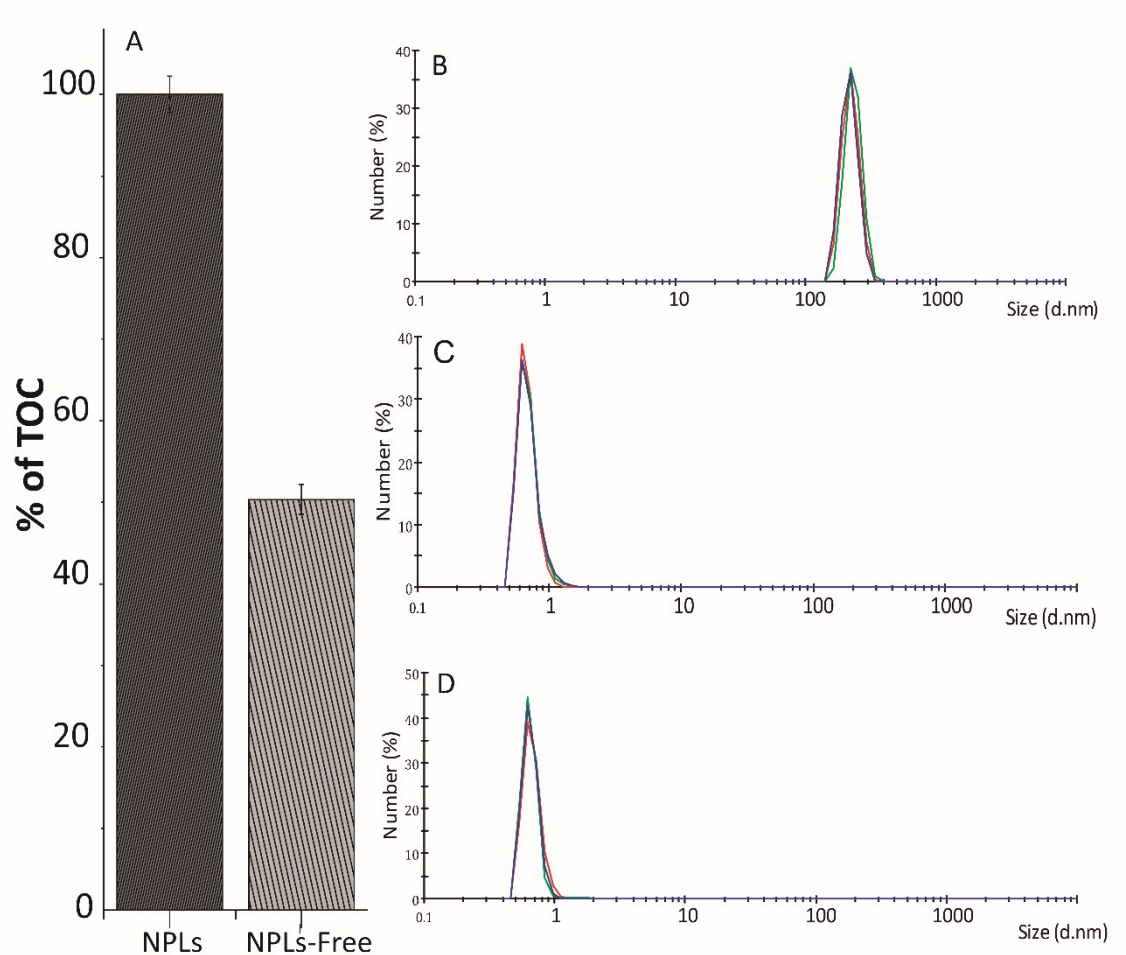


Fig. S4. Physicochemical characterization of the PHB-nanoplastics suspension (obtained from the supernatant of 50 mg/ml of PHB-microplastics abiotically degraded in MilliQ water buffered with 2 mM phosphate (pH 7.0) at 28 °C in constant shaking for 3 days) before and after ultrafiltration by 50 KDa MWCO (pore size of approximately 4 nm). The amount of particulate matter removed by ultrafiltration was measured by comparing the total organic carbon (TOC) before and after the ultrafiltration and was expressed as the percentage that remains in the ultrafiltered solution with respect to the non-ultrafiltered one (A). Size distribution by DLS was also analyzed before ultrafiltration (B), displaying a size of around 200 nm (done by triplicate), and after the ultrafiltration (C) showing a size less than 1 nm, essentially equal to that observed after ultrafiltration of the MilliQ water buffered with 2mM of phosphate (pH 7.0).

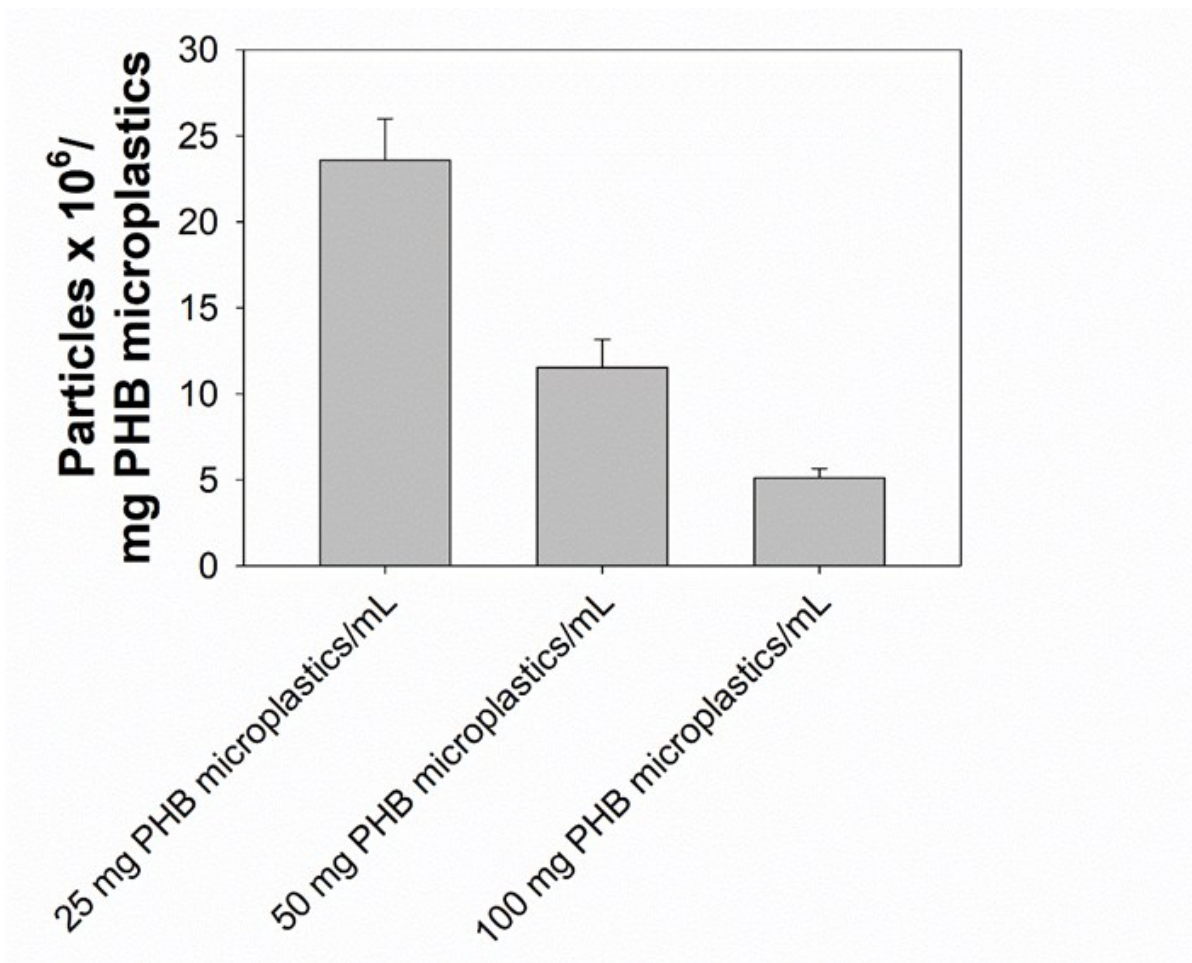


Fig. S5. The total number of formed PHB-NPLs per unit mass of PHB-microplastic after 3 days of abiotic degradation measured by NTA.

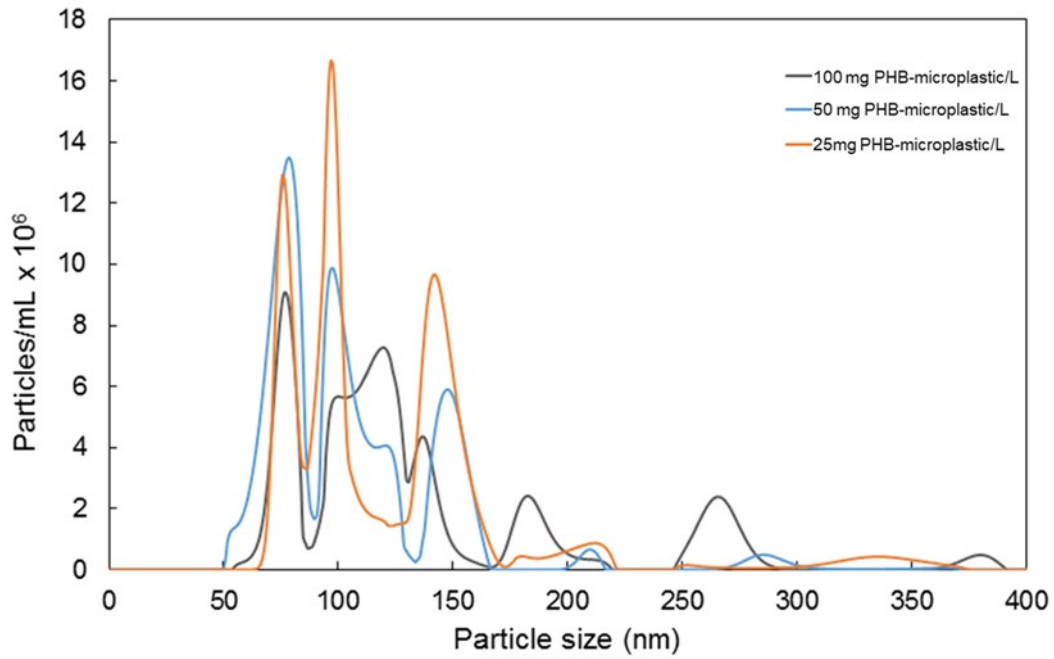


Fig. S6. NTA size distribution of PHB-NPLs obtained from different initial concentration of PHB-microplastics (25, 50 and 100 mg/L) after 3 days of abiotic degradation. MilliQ blank signal was subtracted from the samples.

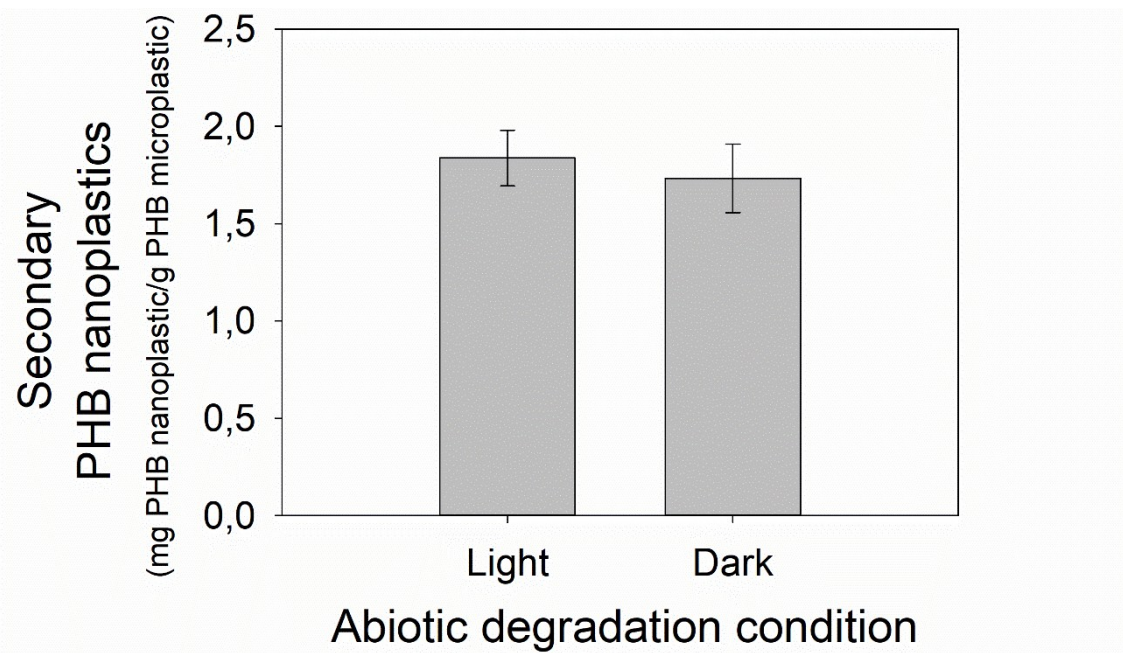


Fig. S7. Secondary PHB nanoplastics released from PHB microplastics (50 mg/mL) after 3 days of the abiotic degradation process under light (ca. 65 $\mu\text{mol photons m}^{-2} \text{s}^{-1}$) and dark. No significant differences were found ($p > 0.05$).

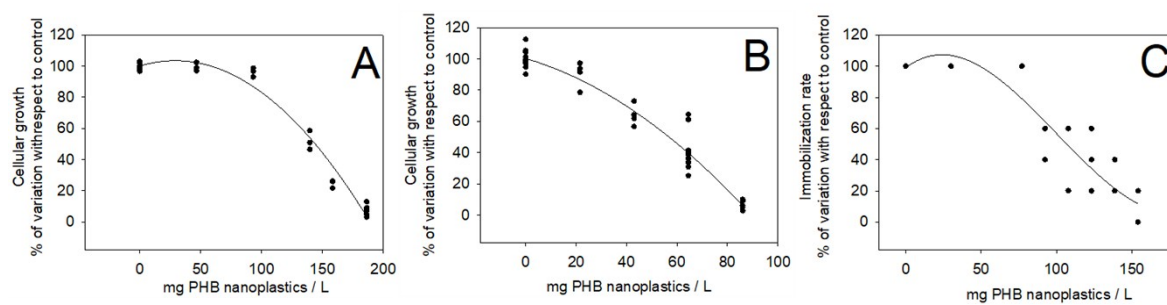


Fig. S8. Dose-response curves of increasing PHB-NPLs concentrations on cellular growth (OD_{750nm}) of *Anabaena* sp. PCC7120 (A) and *Chlamydomonas reinhardtii* (B) cells and immobilization rate of *Daphnia magna* (C) after 3 days of exposure. Results are shown as percentage of variation of growth or immobilization rate \pm SD with respect to controls.

Table S1: Properties of the polyhydroxybutyrate monomer

Polyhydroxybutyrate (PHB)	
Molecular weight	86 g/mol
Formula	C ₄ H ₆ O ₂
Chemical structure	
Estimation of the PHB-nanoplastics concentration using the ratio: C per PHB molecule	The mg of PHB nanoplastics per L were calculated from mg of TOC using the ratio of C per PHB molecule: $(12 \text{ u} \times 4\text{C}) / ((12 \text{ u} \times 4\text{C}) + (1\text{u} \times 6\text{H}) + (16 \text{ u} \times 2\text{O})) = 0.558 \text{ mg of C per mg of PHB}$. Despising the functional groups that could appear after the production of PHB-nanoplastics from PHB-microplastics

Table S2. Used fluorochromes to evaluate the physiological parameters.

Fluorochrome	Applications	Mode of action	Final concentration <i>Anabaena</i> sp. PCC7120	Final concentration <i>Chlamydomonas</i> <i>reinhardtii</i>	Final concentration <i>Daphnia magna</i>
DCFH	General ROS	DCFH is a chemical indicator that diffuses freely into the cells. Once that it enters the cell, esterases cleave the ester bond and turns to highly fluorescent 2',7'-dichlorofluorescein upon oxidation. Therefore, DCFH are used to detect oxidative products in cells. (recorded in FL1 channel)	100 μ M	50 μ M	100 μ M
DHR123	Intracellular levels of hydrogen peroxide	DHR123 passively diffuses across cell membranes. Once that it enters the cell, it can be oxidized, mainly by H ₂ O ₂ , in a slow reaction unless catalyzed by an enzyme with peroxidase activity, and secondarily by peroxyxynitrite anion, to form cationic rhodamine 123. This is a fluorescent compound which localizes in the mitochondria emitting a bright fluorescent signal (recorded in FL1 channel)	10 μ g/mL	10 μ g/mL	-
PI	Membrane integrity	Due to its polarity, PI is unable to pass through intact cell membranes. However, when the integrity of the cell membranes is damaged, PI is able to enter and to intercalate with double-stranded nucleic acids to produce red fluorescence (recorded in FL3 channel)	5 μ g/mL	2.5 μ g/mL	10 μ g/mL
DiBAC ₄ (3)	Cytoplasmic membrane potential	DiBAC ₄ (3) is lipophilic and shows high fluorescence dynamics upon changes in membrane potential by its Nernstian distribution between the inner and outer medium of the cells. Once the cells are equilibrated with DiBAC ₄ (3), depolarization increases fluorescence (recorded in FL1 channel) when is the cells are excited with blue light (488nm excitation laser) as the negatively charged oxonol moves into the cells, where it is bound to intracellular proteins and membranes. Hyperpolarization decreases fluorescence (recorded in FL1 channel). Due to their overall negative charge, it is excluded from the mitochondria, so the mitochondrial membrane potential do not interfere the cytoplasmic membrane potential	2.5 μ g/mL	0.5 μ g/mL	-
BCECF	Intracellular pH	BCECF-AM AM diffuses through the cell membrane and intracellular esterases cleave the ester bond, releasing BCECF. When BCECF AM is excited by blue light (488nm excitation laser), this fluorochrome emits fluorescence with a maximum at 525 nm. In the range of physiological pH, the emission intensity increases with increasing pH. The fluorescence emitted at 620 nm is not pH-dependent. In spite of this wavelength, it is not really an isosbestic point. The ratio of fluorescence emitted at 525 and 620 nm (green/red) was used to analyze pH in cells stained with BCECF	5 μ g/mL	5 μ g/mL	10 μ g/mL
JC-1	Mitochondrial membrane potential	JC-1 exhibits potential-dependent accumulation in mitochondria and owns dual emission potential-sensitive. Fluorescence emission shifts from green (recorded in FL1 channel) to red (recorded in FL2 channel). Mitochondrial depolarization decreases the red/green fluorescence intensity ratio	-	5 μ g/mL	40 μ g/mL

Table S3. DLS diameter and ζ -potential of PHB-NPLs particles released in the abiotic degradation experiment from different initial concentration of PHB-microplastics after 3 days.

Initial concentration of PHB-microplastics	25 mg PHB microplastics / mL	50 mg PHB microplastics / mL	100 mg PHB microplastics / mL
DLS diameter (nm)	209 ± 17	204 ± 22	225 ± 37
ζ-potential at pH 7.0 (mV)	-19.1 ± 2.3	-19.7 ± 3.4	-20.7 ± 3.4